

Published in final edited form as:

*Acta Biomater.* 2011 June ; 7(6): 2384–2393. doi:10.1016/j.actbio.2011.01.016.

## Synthesis and characterization of photocrosslinkable gelatin and silk fibroin interpenetrating polymer network hydrogels

Wenqian Xiao<sup>a,b,c</sup>, Jiankang He<sup>a,b,d</sup>, Jason W. Nichol<sup>a,b</sup>, Lianyong Wang<sup>a,b,e</sup>, Ché B. Hutson<sup>a,b</sup>, Ben Wang<sup>a,b</sup>, Yanan Du<sup>a,b</sup>, Hongsong Fan<sup>c</sup>, and Ali Khademhosseini<sup>a,b,\*</sup>

<sup>a</sup> Center for Biomedical Engineering, Department of Medicine, Brigham and Women's Hospital, Harvard Medical School, 65 Landsdowne Street, Cambridge, MA 02139, USA

<sup>b</sup> Harvard-MIT Division of Health Sciences and Technology, Massachusetts Institute of Technology, Cambridge, MA 02139, USA

<sup>c</sup> National Engineering Research Center for Biomaterials, Sichuan University, Chengdu, Sichuan, PR China

<sup>d</sup> State Key Laboratory of Manufacturing Systems Engineering, Xi'an Jiaotong University, Xi'an, Shanxi, 710049, PR China

<sup>e</sup> Key Laboratory of Bioactive Materials, Ministry of Education, Nankai University, Tianjin, 300071, PR. China

### Abstract

To effectively repair or replace damaged tissues, it is necessary to design scaffolds with tunable structural and biomechanical properties that closely mimic the host tissue. In this paper, we describe a newly synthesized photocrosslinkable interpenetrating polymer network (IPN) hydrogel based on gelatin methacrylate (GelMA) and silk fibroin (SF) formed by sequential polymerization, which possesses tunable structural and biological properties. Experimental results revealed that IPNs, where both the GelMA and SF were independently crosslinked in interpenetrating networks, demonstrated a lower swelling ratio, higher compressive modulus and lower degradation rate as compared to the GelMA and semi-IPN hydrogels, where only GelMA was crosslinked. These differences were likely caused by a higher degree of overall crosslinking due to the presence of crystallized SF in the IPN hydrogels. NIH-3T3 fibroblasts readily attached to, spread, and proliferated on the surface of IPN hydrogels as demonstrated by F-actin staining and analysis of mitochondrial activity (MTT). In addition, photolithography combined with lyophilization techniques was used to fabricate 3D micropatterned and porous micro-scaffolds from GelMA-SF IPN hydrogels, furthering their versatility for use in various microscale tissue engineering applications. Overall, this study introduces a class of photocrosslinkable, mechanically robust and tunable IPN hydrogels that could be useful for various tissue engineering and regenerative medicine applications.

### Keywords

Hydrogel; Silk fibroin; Gelatin; Interpenetrating polymer networks; Photocrosslinking

---

\*Corresponding author. Tel.: 1-617-768-8395, Fax: 1-617-768-8477, alik@rics.bwh.harvard.edu.

**Publisher's Disclaimer:** This is a PDF file of an unedited manuscript that has been accepted for publication. As a service to our customers we are providing this early version of the manuscript. The manuscript will undergo copyediting, typesetting, and review of the resulting proof before it is published in its final citable form. Please note that during the production process errors may be discovered which could affect the content, and all legal disclaimers that apply to the journal pertain.

## 1. Introduction

There is an extensive number of diseases and injuries that lead to tissue degeneration, organ dysfunction and organ failure. While organ/tissue transplants can be an option in some cases, organ recipients often far outnumber organ donors. The fields of tissue engineering and regenerative medicine hold the promise to overcome this outstretched demand through tissue regeneration, organ repair and/or replacement [1]. The current tissue engineering paradigm is typically focused on regenerating tissue with scaffolds seeded with cells in combination with growth factors [2]. Recently, scaffold designs for tissue engineering have focused on mimicking the natural extracellular matrix (ECM)[3]. However, the ECM is not a uniform material; its constituents vary throughout the body in order to meet local environmental, mechanical and structural demands of the body. Thus, tissue engineering scaffolds, like the ECM should have tunable biophysical properties in order to meet tissue specific applications [4].

Hydrogels are one category of scaffold that have been widely used in tissue engineering and regenerative medicine [5]. Some reasons for their popularity are structural similarity to the natural ECM, high water content, biocompatibility and good diffusive properties with respect to oxygen, nutrients and waste products [6–8]. The physical, chemical and biological properties of hydrogels can be easily modulated by varying the degree of crosslinking [9–11] and the combination of materials [12–14]. The result is a series of composite biomaterials that can be tailored to meet the specific mechanical and functional requirements of the host tissues, while promoting tissue morphogenesis.

Hybrid hydrogels are biomaterial systems composed of at least two different hydrogel components, interconnected via chemical or physical means [15]. IPN hydrogels are one type of hybrid hydrogels composed of two or more incompatible crosslinked polymers, where each polymer is either a physically or chemically crosslinked network which is intertwined with, but not crosslinked to, the other polymer(s)[16]. As a hybrid hydrogel, the IPN hydrogels could share the properties of each polymer in the network. Furthermore, the highly entangled networks often result in a mechanically reinforced and strengthened hydrogel system [13].

Gelatin methacrylate (GelMA) is formed by incorporating methacrylate groups onto the amine-containing side groups of gelatin, yielding a gelatin-based, photocrosslinkable hydrogel [17]. Comprised of degraded natural ECM components, GelMA can form covalently and irreversibly crosslinked hydrogels through exposure to UV light in the presence of a photoinitiator [9,17–19]. Recently, GelMA has been demonstrated as a useful tissue engineering hydrogel system that promotes cell proliferation, migration and spreading both in 2D [9] and 3D [9,18,19] and is compatible with microfabrication techniques for creating cell-laden microtissues [9,19]. Although GelMA hydrogels have many advantageous properties, such as low cost, ease of production, natural cell binding and degradation motifs, for materials requiring long degradation times or greater mechanical stiffness its suitability may be limited.

Silk fibroin (SF) derived from *Bombyx mori* is a self-assembling structural protein which possesses many important material properties for tissue engineering and regenerative medicine, such as good mechanical strength, biocompatibility, high dissolved-oxygen and water-vapor permeability, and resistance to enzymatic degradation [20–24]. SF is comprised of a heavy polypeptide chain and a light chain. The heavy chains consist primarily of Gly-Ala-Gly-Ala-Ser residues which can be formed the  $\beta$ -sheet secondary crystalline structures [25,26]. As compared to other polymers, an important advantage of SF for hydrogel systems is its ability to physically crosslink without any chemical modifications. The gelation of SF

is the process of protein aggregation which was related to the conformational change of the SF molecules from a random coil to  $\beta$ -sheet [27]. The properties of mechanical and degradation of hydrogel are largely influenced by the crystallinity and degree of physical crosslinking [28].

In this paper, we report the synthesis and characterization of IPN hydrogels consisting of sequentially polymerized GelMA and SF. It was hypothesized that sequential crosslinking of GelMA, followed by SF network formation would yield a tunable, hybrid hydrogel with good cell biocompatibility and mechanical properties for tissue engineering. We tested the hypothesis that mixed prepolymer GelMA-SF solutions exposed to UV light in the presence of a photoinitiator would photocrosslink only the GelMA, while immobilizing the amorphous SF. Subsequent exposure to aqueous methanol (MeOH) was used to test the induction of SF crystallization in polymerized GelMA-SF hydrogels to form crystalline  $\beta$ -sheets which acted as a reinforcement component. Further variation of the concentration of SF tested the tunability of the resulting series of IPN hydrogels from biophysical, structural and cell compatibility perspectives. Lastly, to explore the applicability of these IPN networks to the microscale tissue engineering field, we investigated the fabrication of 3D micro-scaffolds and assessed their cytocompatibility. The resulting IPN micro-scaffold systems could be used to make functional micro-tissues for use in “bottom-up” assembly of biomimetic engineered tissues [29].

## 2. Materials and methods

### 2.1. Materials

Raw silk fiber was purchased from Siyuan Textile Company (Tong Xiang, Zhejiang, China). The photoinitiator, 2-hydroxy-1-[4-(hydroxyethoxy)-phenyl]-2-methyl-1-propanone (Irgacure 2959) was obtained from Ciba Geigy (Dover, NJ). The Live/Dead Viability/Cytotoxicity kit, Alexa Fluor 594-labelled phalloidin and DAPI were ordered from Invitrogen Corporation (Invitrogen, Carlsbad, USA). Collagenase type II was purchased from Worthington Biochemical Corporation (Lakewood, NJ, USA). The OmniCure® S2000 UV/Visible Spot Curing System from EXPO Photonic Inc (Ontario, Canada) was used for polymerization of hydrogels. All other chemicals were purchased from Sigma-Aldrich (St. Louis, USA) unless specifically mentioned.

### 2.2. Silk-fibroin (SF) purification and concentration

SF aqueous stock solutions were prepared as previously described [30]. First, to remove the sericin coating (degum), the silk fiber was boiled in aqueous solution with 0.25% (w/v) sodium dodecylsulfate (SDS) and 0.25% (w/v) sodium carbonate for 1 hour, with the raw silk added at a ratio of 1:100 w/v. The degummed silk fiber was thoroughly rinsed with deionized water. The washed fiber was air-dried and dissolved in 9.3M Lithium bromide (LiBr) solution at 60°C for 4 hour to make a 20% (w/v) solution. The solution was dialyzed against deionized water in a 3500Da cutoff dialysis tube (VWR Scientific) for 3 days at 4°C, and was further purified by centrifuging at 8,000 rpm for 20 minutes. To obtain silk solutions with higher concentrations, the SF solution was concentrated in a 3500 Da cutoff dialysis tube (VWR Scientific) against 20% (w/v) PEG (10,000 g/mol) solution for 24 hours at 4°C. The final concentration of the aqueous SF solution was adjusted to 8 wt%, which was determined by weighing the remaining solid after drying. The solution was either directly used or stored at 4°C for future use.

### 2.3. Synthesis of gelatin methacrylate (GelMA)

GelMA was synthesized as described previously [9,17]. Type A gelatin derived from porcine skin (Sigma-Aldrich) was dissolved in Dulbecco's phosphate buffered saline

(DPBS, GIBCO, CA) at 60°C to make a 10 wt% uniform solution. 5 ml of methacrylic anhydride (MA) was added to the gelatin solution at a rate of 0.5 ml/min under stirring conditions (Fig. 1A). The mixture was allowed to react at 50°C for 3 hours. After a 5× dilution with additional warm DPBS, the GelMA solution was dialyzed against deionized water using a 12–14 kDa cutoff dialysis tube (VWR Scientific) for 6 days at 50°C to remove unreacted methacrylic anhydride and additional by-products. The GelMA solution was frozen at –80°C, lyophilized and stored at –80°C until further use. The percent methacrylation of the gelatin used in these experiments is roughly 73% as characterized by NMR [9].

#### 2.4. Preparation of GelMA-SF composite hydrogels

The prepolymer solution was prepared by mixing 6 wt% GelMA solution with 0.5, 1 and 2 wt% SF to produce the G-S-0.5, G-S-1 and G-S-2 hydrogel prepolymer solutions (Table 1). The photoinitiator was added to the prepolymer solutions for a final concentration of 1 wt%. GelMA-SF prepolymer solutions were vigorously stirred at room temperature for 10 minutes to generate a homogeneous solution. Fig. 1B shows the schematic diagram of the synthesis process, to fabricate GelMA-SF IPN hydrogels. Briefly, 150 µL prepolymer solution was pipetted into the cylindrical poly(dimethylsiloxane) (PDMS) mold covered on a 3-(trimethoxysilyl)propyl methacrylate (TMSPMA) treated glass slide, and then exposed to UV light (320–500nm, 7.0 mW/cm<sup>2</sup>) for 2 minutes to allow for free radical polymerization of GelMA chains by photocrosslinking. After being detached from the mold, the resulting GelMA-SF semi-IPN hydrogels were treated with 70% (v/v) MeOH aqueous solution for 1 hour at room temperature. The GelMA-SF IPN hydrogels were removed from the glass slide and rinsed thoroughly with DPBS to remove residual of methanol.

#### 2.5. Swelling ratio measurement

To assess gel swelling, the GelMA-SF composite hydrogels were immersed in DPBS at room temperature for 24 hours. After excess surface water was removed with filter paper, the swollen weight of each hydrogel was recorded. The samples were then frozen and lyophilized to obtain the hydrogel dry weight. The swelling ratio for each hydrogel was calculated as the ratio of wet mass to dry mass. The sample size was 4 gels per group.

#### 2.6. Mechanical testing

The mechanical properties of the GelMA-SF composite hydrogels were characterized by compressive stress–strain measurements on an Instron 5542 mechanical tester at room temperature. The hydrogel sample, 6.7 mm in diameter and 1.5 mm in height, was tested at a rate of 20% strain/min. The compressive modulus was determined as the slope of the linear region of the stress-strain curve corresponding with 0–10% strain. The sample size was 3 to 4 gels per group.

#### 2.7. *In vitro* enzymatic degradation

To characterize the enzymatic degradation properties of GelMA-SF IPN hydrogels, the hydrogel samples were placed in 1.5 ml centrifuge tubes with 1ml DPBS containing 1 – 2 U/ml collagenase type II at 37°C. At a pre-defined time, the hydrogels for each condition were removed, frozen, and lyophilized. The mass loss was determined by the ratio of final weight to the original dry weight. The sample size was 5 gels per group.

#### 2.8. SEM characterization

To characterize the internal microstructures of the GelMA-SF composite hydrogels, the swollen hydrogel samples were frozen at –80°C and then lyophilized. The dried hydrogels were cut to expose the cross-sections and coated with Pt/Pd using a sputter coater (SP-2 AJA

Sputtering System). The samples were observed by using scanning electron microscopy (SEM, Zeiss Ultra 55, Germany) under an accelerating voltage of 15 kV. The ImageJ software was used to quantify the porosity based on the SEM pictures [31]. At least 5 images from 3 samples for each group were used for the quantification.

## 2.9. Cell culture

NIH-3T3 fibroblasts were maintained in Dulbecco's modified eagle medium (DMEM; Gibco) supplemented with 10% FBS and 1% penicillin/streptomycin, and were cultured in a standard cell culture incubator (Forma Scientific) in a 5% CO<sub>2</sub> atmosphere at 37°C. The cell culture media was changed every 2 days and cells were passaged twice a week.

## 2.10. Cell morphology on GelMA-SF IPN hydrogels

To investigate the effect of GelMA-SF IPN hydrogels with different SF concentrations on cell behavior (proliferation and spreading), the NIH-3T3 fibroblasts were seeded at a density of  $1.3 \times 10^4$  cells/cm<sup>2</sup> on the surface of the hydrogels. The culture media was changed every day. After 1 and 3 days culture, the hydrogel samples were fixed in 3.7% paraformaldehyde solution, treated with 0.1% Triton X-100 and stained with Alexa Fluor 594 phalloidin and counterstained with DAPI to facilitate cell number counting. The samples were visualized with a fluorescent microscope (Nikon Eclipse TE 2000-U, AVON, MA). ImageJ software was used to quantify cell number and single cell spreading area from fluorescence images. At least six images from 3 samples for each group were used for quantification of the cell number and spreading area.

## 2.11. Cell metabolic activity studies

Cell metabolic activity on the surface of GelMA-SF IPN hydrogels was analyzed with an MTT colorimetric assay. 100 µl of hydrogel prepolymer solution was added to each well of a 48-well plate. After UV exposure (7.0 mW/cm<sup>2</sup>) for 2 minutes, the samples were treated with 70% (v/v) MeOH solution, and then thoroughly rinsed with sterilized DPBS solution. 500 µl of NIH-3T3 fibroblast cells suspension was seeded on the hydrogel surface at a density of  $1.5 \times 10^4$  cells/well. The culture media was changed every day. At predetermined times, 500 µl of 5 mg/ml 3-(4,5-Dimethylthiazol-2-Yl)-2,5-Diphenyl tetrazolium Bromide (MTT) solution was added to each wells. After 4 hours of incubation, the supernatant was carefully removed and 500 µl of dimethyl sulfoxide (DMSO) solution was added to dissolve the formazan crystals. After shaking for 10 minutes on a plate mini shaker, 100 µl solution was transferred into a 96-well plate and the absorbance was read at 570 nm with the reference wavelength 650 nm by Epoch Microplate Spectrophotometer (BioTek, Winooski, VT). Five parallels were averaged for each hydrogel sample.

## 2.12. Microfabrication of GelMA-SF IPN hydrogels

To fabricate micropatterned GelMA-SF composite porous scaffolds, photomasks with square patterns (dimensions: 700 × 700 µm) were designed using AutoCAD and printed on transparencies with 20,000-dpi resolution (CAD/Art Services). To fabricate the microgels, 100 µl of G-S-0.5 prepolymer solution was pipetted onto a flat hydrophobic PDMS molds covered by a TMSPPMA treated glass side separated by two cover slips which makes a 300 µm space in the middle, the photomask was placed on the top of glass slide and the prepolymer was exposed to UV light for 30 seconds (7.0 mW/cm<sup>2</sup>). The GelMA-SF semi-IPN hydrogel patterns were then rinsed with DPBS to remove excess prepolymer then the hydrogel pattern was immersed into 70% (v/v) MeOH solution for 1 hour. The glass slide with patterned hydrogels were frozen at -80°C for 2 hours and then lyophilized. The micropatterned scaffolds were coated with Pt/Pd and were observed with the SEM under an accelerating voltage of 15 kV. The micropatterned scaffolds were treated by ethanol series

(100%, 75%, 50% and 25% (v/v)) as previously described to prevent deforming of the scaffold [32]. The micro-scaffolds were washed with the sterile DPBS, put in 4-well plates and filled with 5 ml of cell suspension containing  $1 \times 10^5$  cells per ml for each well. These plates were cultured in a 5% CO<sub>2</sub> atmosphere at 37°C incubator. After one day culture, cells were stained with live/dead viability kit and visualized under a fluorescence microscope.

### 2.13. Statistical analysis

Hydrogel data were analyzed by using one-way and two-way analysis of variance (ANOVA) with SF concentration, methanol treatment and time in culture as independent variables. Post hoc analysis was performed with Fisher's LSD test. Statistical analysis was performed with GB-STAT v8.0 (Dynamic microsystems, Silver Springs, MD). For all statistical tests, the level of significance was set at  $p < 0.05$ . Data are presented as mean  $\pm$  standard deviation (SD).

## 3. Results

### 3.1. Swelling properties

All the hydrogels (IPNs, semi-IPNs and GelMA hydrogels) were generated as previously described and allowed to reach equilibrium with 24 hour incubation in DPBS at room temperature. Hydrogels were then weighed and lyophilized. Wet and dry weights were used to generate the swelling ratio. A two-way ANOVA revealed a significant effect of MeOH treatment ( $p < 0.05$ ), SF concentration ( $p < 0.05$ ) and an interactive effect between MeOH treatment and SF concentration ( $p < 0.05$ ) on the swelling properties of the composite hydrogels. These analyses illustrated that supplementing GelMA hydrogels with SF significantly reduces the swelling ratio of GelMA-SF semi IPN hydrogels. Furthermore, the interaction exhibited that the addition of SF in combination with MeOH treatment significantly reduces the swelling ratio more than SF supplementation or MeOH treatment alone. It is known that treatments with aqueous MeOH solution induce a conformational transformation of SF from random coils to  $\beta$ -sheets, which introduces more physical crosslinking sites in the hydrogel network [33]. Moreover, the crystallized SF in the hydrogel network is impermeable to water, decreasing the swelling ratio of IPN hydrogels [34]. For semi-IPN hydrogels, the SF is entangled in the GelMA network, resulting in a relatively loose structure with a higher swelling ratio.

### 3.2. Mechanical properties

We also evaluated the effects of SF concentration and crystallization on the mechanical properties of GelMA hydrogels by using an unconfined, uniaxial compression test. Statistical analysis illustrated a significant effect of SF concentration ( $p < 0.05$ ), MeOH treatment ( $p < 0.05$ ) and an interactive effect between SF concentration and MeOH treatment ( $p < 0.05$ ) on the compressive modulus of the hydrogels (Fig. 3). These results displayed the ability of SF concentration and MeOH treatment to individually affect the compressive modulus of hydrogels. Furthermore, the interaction described the ability of SF concentration in combination with MeOH treatment to result in a synergistic effect on the compressive modulus, enhancing the compressive modulus of the GelMA-SF hydrogels more than an increase SF concentration or MeOH treatment alone. Post hoc analysis did not reveal significant alterations in the compressive modulus of GelMA-SF semi-IPN hydrogels when compared to GelMA alone. However, treatment with a 70% (v/v) MeOH solution significantly increased the compressive modulus of the GelMA-SF hydrogels compared to both GelMA alone and GelMA-SF semi-IPN hydrogels; increasing the concentration of SF from 0.5 to 2 wt% increased the compressive modulus by almost 5-fold. We hypothesize that MeOH treatment for the GelMA-SF composite hydrogel could induce  $\beta$ -sheet formation, which form a reinforced microstructure and increase the crosslinking degree.

### 3.3. Degradation profile

The enzyme mediated degradation profiles of GelMA-SF IPN hydrogels were investigated using collagenase solutions *in vitro*. Statistical analysis demonstrated a significant effect of culture time ( $p < 0.05$ ), SF concentration ( $p < 0.05$ ) and an interactive effect between culture time and SF concentration ( $p < 0.05$ ) on the degradation profiles of composite hydrogels at both 1 U/ml and 2 U/ml of collagenase (Fig. 4). Overall statistical analyses revealed that the addition of SF significantly reduces the degradation rate of GelMA-SF IPN hydrogels irrespective of the collagenase concentration, resulting in an inverse correlation between SF concentration and degradation rate of GelMA-SF IPN hydrogels. The significant effect of culture time confirmed that the longer the hydrogels are in culture the greater the mass loss. The degradation results can be attributed to the more compact structure of IPN hydrogels and the presence of  $\beta$ -sheet structures, which can act as water insoluble backbones, hindering the permeation of collagenase solution into hydrogel [35]. There was no significant weight loss observed in PBS controls for all the IPN hydrogels after 72 hours.

### 3.4. Interior morphology of Gel-MA/SF composite hydrogel

To better understand the structure–function relationship of the GelMA-SF composite hydrogels, we examined the corresponding cross-sectional microstructures of hydrogels by SEM (Fig. 5A). The Fig. 5B shows the porosity based on the SEM images. The GelMA and GelMA-SF semi IPN hydrogels with 0.5 wt% SF showed a loose, honey-comb-like structure (Fig. 5A1 and 5A2). With the addition of 1 wt% and 2 wt% SF (Fig. 5A4 and 5A6), the semi-IPN hydrogels displayed some parallel sheet structures as SF formed sheet-like morphology during the freezing process [36], and there were no significant difference of the porosity between all the Semi-IPN hydrogels. After MeOH treatment, for the G-S-0.5 IPN, the wall thickness of material surrounding the pores was greater than in semi-IPN hydrogels, although the porous structure was retained (Fig. 5A3). For the G-S-1 and G-S-2 IPN hydrogel (Fig. 5A5 and 5A7), the porosity have decreased to 54% and 41.8%, respectively and the sheet structure became more visible when more SF added. From the SEM images, no visible phase separation was observed for all groups of GelMA-SF composite hydrogels.

### 3.5. Cell morphology on GelMA-SF IPN hydrogels

The ability of cells to attach, spread, and proliferate on hydrogels are important attributes for tissue development. To investigate the effects of SF supplementation on cellular adhesion and proliferation, NIH-3T3 fibroblasts were seeded on IPN hydrogels and stained with fluorescently-labeled phalloidin and DAPI to visualize F-actin fibers and cell nucleus respectively (Fig. 6A). We evaluated the single cell spreading area and the total cell area (cells/mm<sup>2</sup>) on the surface of GelMA-SF IPN hydrogels. For single cell spreading area after 1 day in culture, statistical analysis revealed no significant differences between groups ( $p > 0.05$ ) (Fig. 6B) demonstrating that the addition of SF does not affect the ability of cells to spread on GelMA-SF IPN hydrogels. For cellular attachment and proliferation on the GelMA-SF IPN hydrogel surface, a two-way ANOVA revealed a significant effect of SF concentration ( $p < 0.05$ ), culture time ( $p < 0.05$ ) and an interactive effect between SF concentration and culture time ( $p < 0.05$ ) on the number of cells/mm<sup>2</sup> on the hydrogels (Fig. 6C). Overall these statistical results illustrated that NIH-3T3 cells can proliferate on all GelMA-SF IPN hydrogels over 3 days and that increasing the concentration of SF reduces NIH-3T3 proliferation rate. Post hoc analysis found no significant differences between GelMA-SF IPN hydrogels and GelMA alone on the number of cells per square millimeter after 1 day in culture. After 3 days in culture, 0.5% SF supplementation significantly enhanced the number of cells per square millimeter compared to GelMA alone, as the substrate stiffness could affects fibroblast proliferation. However, higher concentrations of SF reduced the number of cells per square millimeter suggesting that the higher degree of  $\beta$ -sheet formation on the hydrogel surface is less favorable for cell proliferation [37].

Nonetheless, GelMA-SF IPN hydrogels displayed tunable adhesion and proliferation rate profiles.

### 3.6. Cell metabolic activity on GelMA-SF IPN hydrogel

The MTT assay was implemented to quantitatively investigate cell metabolic activity of NIH-3T3 cells on GelMA-SF IPN hydrogels after 1, 3, and 5 days in culture. As shown in Fig. 7, the statistical analysis illustrated a significant effect of SF concentration ( $p < 0.05$ ), culture time ( $p < 0.05$ ) and an interactive effect between SF concentration and culture time ( $p < 0.05$ ) on cell metabolic activity. These results revealed that NIH-3T3 cells had an increased metabolic activity on all GelMA-SF IPN hydrogels over 3 days and that increasing the concentration of SF reduced NIH-3T3 metabolic activity. After 1 day in culture, Fischer's LSD post hoc analysis illustrated that the cellular metabolic activity was statistically indistinguishable between the hydrogels. However, after 3 and 5 days of culture, MTT assay revealed the highest metabolic activities for pure GelMA hydrogels and GelMA-SF IPN with 0.5% SF. In general, the cell metabolic activity matched the attachment and proliferation data in Fig. 6. The MTT assay measures the ability of mitochondrial enzymes to reduce MTT, thus the more cells attached to the hydrogel surface, the more cells present and a higher metabolic measurement from the assay.

### 3.7. Gel-MA/SF composite materials for micropatterned porous scaffolds

To demonstrate the advantage of GelMA-SF IPN hydrogels for microscale tissue engineering applications, we employed photolithography and freeze drying methods to engineer micropatterned porous scaffolds. GelMA-SF composite material with 0.5% SF (G-S-0.5) was chosen as it displayed desirable mechanical and degradation properties yet retained similar biological properties as pure GelMA. The micro-patterned scaffolds exhibited open and interconnected porous structures, a feature that is imperative for tissue engineered scaffolds (Fig. 8B). However, for the micropatterned Gel-MA scaffolds, we found there was a thin superficial film that covered the porous structures (Fig. S1), which was previously observed for the gelatin scaffolds prepared by freeze-drying method [38]. Live/Dead images of NIH-3T3 cells cultured on the micropatterned scaffolds for one day display a high rate of viability and uniform distribution. It is envisioned that these microscale scaffolds could be seeded with different types of cells and then harvested to assemble into heterogeneous tissue grafts using a "bottom-up" approach [29].

## 4. Discussion

Here, we have synthesized a photocrosslinkable protein-based hydrogel composed of gelatin methacrylate and silk fibroin. Both gelatin and SF extracted from the *Bombyx mori* silkworm are FDA approved for specific applications and have been widely used in tissue engineering and regenerative medicine applications. Gelatin is obtained by breaking the triple-helix structure of collagen into single-stranded macromolecules. When in solution, gelatin molecules form reversible hydrogels inversely proportional to temperature, which are not stable at normal body temperature of 37°C due to gelatin's relatively low melting point. Many methods exist to crosslink gelatin to make the properties of gelatin hydrogels more temperature stable, such as treatment with glutaraldehyde [39], carbodiimides [40] or genipin [41,42]. Recently, photocrosslinkable gelatin methacrylate (GelMA) hydrogels have gained much attention in the tissue engineering field [9,17–19]. One of most important advantages of GelMA is its compatibility with microfabrication techniques that could lead to the development of stem cell niches [43] or tissue engineered constructs that can be spatially customized [19,44]. All gelatin-based hydrogels have the innate advantage of the cell responsivity of gelatin; however, 3D encapsulation is only compatible with some crosslinking techniques.

The physical and chemical properties of SF largely depend on its molecular conformation and crystallinity. Crystallization of SF can be readily induced by physical [45,46] and chemical treatments [47]. Methanol is a very widely used organic solvent to induce SF crystallization. When treating with methanol, the chain-chain contact and  $\beta$ -sheet structures are induced due to the dehydration of hydrated hydrophobic domains of SF [47]. Recently, a protein hydrogel based on SF and gelatin was reported [33,34,48], where the gelatin was mixed with SF, and then the MeOH was applied to induce the crystallization of SF. In these studies, there was no phase separation when mixing two polymers and the crystallization of SF was not interfered by the presence of gelatin. Furthermore, the thermal stability and mechanical property of the composite hydrogel were improved by the presence of crystallized SF. A similar phenomenon was observed with SF and GelMA in our study. The major difference for our study is the use of GelMA, rather than pure gelatin, which introduced the photo-polymerization mechanism into the IPN synthesizing process. The GelMA-SF IPN hydrogel was demonstrated to be compatible with common microfabrication technology to create the three dimensional microscale tissue engineering scaffolds.

Hydrogels used for the biomedical field must be versatile to meet different biophysical and biochemical requirements. Mandal et al., have reported a SF/polyacrylamide semi-IPNs hydrogel with the tunable property by varying the ratio of two components for controlled drug release [49]. In our study, a full IPN hydrogel was formed by the sequential polymerization of GelMA and SF; the formation of IPN hydrogels with varying SF concentrations allowed for tunable biophysical properties of the resulting hydrogels. For specific tissue engineering applications, matching the mechanical properties of the polymer scaffold with those of the host tissues is important [50]. The incorporation of SF in the IPN hydrogels increased the compressive modulus as SF acted as a mechanical reinforcement component. By controlling the concentration of SF, the mechanical properties of IPN hydrogel could be tunable across a wide range of mechanical stiffnesses which could meet different requirements of specific host tissues [50]. One of the goals of tissue engineering is to ensure that tissue constructs can be incorporated into the surrounding host tissue. This requires that biopolymer scaffolds degrade at a rate similar with the growth rate of new tissue as a mismatch in these rates can lead to premature failure of the tissue development [25]. Therefore, the degradation rate is an important parameter when designing hydrogel scaffolds for tissue engineering. The degradation profiles clearly demonstrated that GelMA-SF IPN hydrogels had a significantly lower mass loss as compared to pure Gel-MA hydrogels. The degradation rate could be controlled by the amount of crystallized SF in the hydrogels suggesting a degree of degradation tunability. This is particularly useful in biodegradable scaffolds in which slow tissue growth is desirable such as bone or cartilage [51,52]. Although protease XIV have been shown high activity towards the  $\beta$ -sheet structures of SF, the protease XIV is not present in the human body [53,54]. Therefore we chose collagenase solely for its known ability to degrade GelMA and as one of the important degradation enzymes in vivo. Also, SEM characterization revealed that the IPN hydrogels possessed reduced porosity, especially as the SF content increased suggesting the ability to control the porosity for different tissue engineering applications. The results of cell attachment experiments demonstrated that 0.5 wt% SF IPNs were the most suitable for cell spreading and proliferation, however, IPN hydrogels with a higher content of crystallized SF did not demonstrate as favorable cell-biomaterial interactions. The cell proliferation rate decreased as the silk concentration increased, potentially making higher concentrations of SF less desirable for applications requiring rapid cell proliferation. Thus, the physical, chemical and biological properties of the IPN scaffolds could be tailored for specific applications by optimizing the individual concentrations of SF and GelMA, with careful attention paid to the desired cell proliferation required.

By mimicking native microstructural functional units, “bottom-up” approaches aim to create biomimetic engineered tissues by using microscale building blocks to construct modular tissues [29]. Du et al. used the “bottom-up” approach to assemble cell-laden hydrogels to generate tissue constructs [55]. However, because the cells have to be encapsulated into the hydrogel, the UV crosslinking and the residue of photoinitiator could negatively influence cell viability. Here we have presented a novel method to fabricate 3-D micro-scaffolds based on GelMA-SF IPN hydrogels. Based on the G-S-0.5 IPN hydrogel, following photolithography and lyophilization, we obtained 3D, interconnected porous micro-scaffolds which could provide a 3D support structure for cell growth. High porosity and pore connectivity are essential to ensure sufficient nutrient, oxygen and metabolite diffusion throughout the scaffold. Incorporating SF could provide the scaffold with greater structural integrity, stability and insolubility as compared to GelMA alone. For micro-patterned scaffolds, cells attached and grew in the 3D pores throughout the scaffold. Overall, this 3D micro-scaffold could be a substitute for the cell-laden microgel for use in “bottom-up” assembly to create biomimetic tissue engineering constructs.

## 5. Conclusions

In summary, we have synthesized a series of photocrosslinkable GelMA-SF IPN hydrogels with desirable and tunable features for biomedical applications. The GelMA-SF IPN hydrogels have lower swelling ratio, higher Young’s modulus, resistance of collagenase degradation and denser network structures as compared to both semi-IPNs (GelMA crosslinking only) and GelMA hydrogels. We also demonstrated that by varying the concentration of silk fibroin in the IPN hydrogel, the biophysical, structural and biological properties of the resulting IPN hydrogels could be tuned. The tunable GelMA-SF IPN hydrogels are anticipated to constitute an attractive biomaterial to meet different requirements in the tissue engineering field. Finally, we created porous micropatterned scaffolds with GelMA-SF IPN hydrogels and those micro-scaffolds, upon directed assembly, could be used in engineering complex tissue constructs by “bottom-up” approach.

## Supplementary Material

Refer to Web version on PubMed Central for supplementary material.

## Acknowledgments

Wenqian Xiao acknowledges financial support from the China Scholarship Council (CSC). This work was supported by the National Institutes of Health (EB007249; DE019024; HL092836), the NSF CAREER award and the US Army Corps of Engineers. J.W.N. was supported by the U.S. Army Construction Engineering Research Laboratory, Engineering Research and Development Center (USACERL/ERDC). The authors would like to thank Ying-Chieh Chen, Junshan Liu, Shilpa Sant and Gulden Camci-Unal for the scientific and technical support.

## References

1. Langer R, Vacanti JP. Tissue engineering. *Science* (New York, NY). 1993; 260:920–6.
2. Khademhosseini A, Vacanti JP, Langer R. Progress in tissue engineering. *Scientific American*. 2009; 300:64–71. [PubMed: 19438051]
3. Lutolf MP, Lauer-Fields JL, Schmoekel HG, Metters AT, Weber FE, Fields GB, et al. Synthetic matrix metalloproteinase-sensitive hydrogels for the conduction of tissue regeneration: engineering cell-invasion characteristics. *Proceedings of the National Academy of Sciences of the United States of America*. 2003; 100:5413–8. [PubMed: 12686696]
4. Jia X, Kiick KL. Hybrid multicomponent hydrogels for tissue engineering. *Macromolecular bioscience*. 2009; 9:140–56. [PubMed: 19107720]

5. Khademhosseini A, Langer R. Microengineered hydrogels for tissue engineering. *Biomaterials*. 2007; 28:5087–92. [PubMed: 17707502]
6. Peppas NA, Hilt JZ, Khademhosseini A, Langer R. Hydrogels in biology and medicine: From molecular principles to bionanotechnology. *Advanced Materials*. 2006; 18:1345–60.
7. Lee KY, Mooney DJ. Hydrogels for tissue engineering. *Chemical reviews*. 2001; 101:1869–79. [PubMed: 11710233]
8. Hoffman AS. Hydrogels for biomedical applications. *Advanced drug delivery reviews*. 2002; 54:3–12. [PubMed: 11755703]
9. Nichol JW, Koshy ST, Bae H, Hwang CM, Yamanlar S, Khademhosseini A. Cell-laden microengineered gelatin methacrylate hydrogels. *Biomaterials*. 2010; 31:5536–44. [PubMed: 20417964]
10. Coutinho DF, Sant SV, Shin H, Oliveira JT, Gomes ME, Neves NM, et al. Modified Gellan Gum hydrogels with tunable physical and mechanical properties. *Biomaterials*. 2010; 31:7494–502. [PubMed: 20663552]
11. Shin H, Nichol JW, Khademhosseini A. Cell-adhesive and mechanically tunable glucose-based biodegradable hydrogels. *Acta biomaterialia*. 2010
12. Weng L, Gouldstone A, Wu Y, Chen W. Mechanically strong double network photocrosslinked hydrogels from N,N-dimethylacrylamide and glycidyl methacrylated hyaluronan. *Biomaterials*. 2008; 29:2153–63. [PubMed: 18272215]
13. Suri S, Schmidt CE. Photopatterned collagen-hyaluronic acid interpenetrating polymer network hydrogels. *Acta biomaterialia*. 2009; 5:2385–97. [PubMed: 19446050]
14. Liu Y, Chan-Park MB. Hydrogel based on interpenetrating polymer networks of dextran and gelatin for vascular tissue engineering. *Biomaterials*. 2009; 30:196–207. [PubMed: 18922573]
15. Kopecek J. Hydrogel biomaterials: a smart future? *Biomaterials*. 2007; 28:5185–92. [PubMed: 17697712]
16. Brigham MD, Bick A, Lo E, Bendali A, Burdick JA, Khademhosseini A. Mechanically robust and bioadhesive collagen and photocrosslinkable hyaluronic acid semi-interpenetrating networks. *Tissue Eng Part A*. 2009; 15:1645–53. [PubMed: 19105604]
17. Van Den Bulcke AI, Bogdanov B, De Rooze N, Schacht EH, Cornelissen M, Berghmans H. Structural and rheological properties of methacrylamide modified gelatin hydrogels. *Biomacromolecules*. 2000; 1:31–8. [PubMed: 11709840]
18. Benton JA, DeForest CA, Vivekanandan V, Anseth KS. Photocrosslinking of gelatin macromers to synthesize porous hydrogels that promote valvular interstitial cell function. *Tissue engineering*. 2009; 15:3221–30. [PubMed: 19374488]
19. Aubin H, Nichol JW, Hutson CB, Bae H, Sieminski AL, Crokek DM, et al. Directed 3D cell alignment and elongation in microengineered hydrogels. *Biomaterials*. 2010; 31:6941–51. [PubMed: 20638973]
20. Hofmann S, Knecht S, Langer R, Kaplan DL, Vunjak-Novakovic G, Merkle HP, et al. Cartilage-like tissue engineering using silk scaffolds and mesenchymal stem cells. *Tissue Eng*. 2006; 12:2729–38. [PubMed: 17518642]
21. Lovett M, Cannizzaro C, Daheron L, Messmer B, Vunjak-Novakovic G, Kaplan DL. Silk fibroin microtubes for blood vessel engineering. *Biomaterials*. 2007; 28:5271–9. [PubMed: 17727944]
22. Yang Y, Ding F, Wu J, Hu W, Liu W, Liu J, et al. Development and evaluation of silk fibroin-based nerve grafts used for peripheral nerve regeneration. *Biomaterials*. 2007; 28:5526–35. [PubMed: 17884161]
23. Zhang X, Wang X, Keshav V, Wang X, Johanas JT, Leisk GG, et al. Dynamic culture conditions to generate silk-based tissue-engineered vascular grafts. *Biomaterials*. 2009; 30:3213–23. [PubMed: 19232717]
24. Zhang X, Reagan MR, Kaplan DL. Electrospun silk biomaterial scaffolds for regenerative medicine. *Advanced drug delivery reviews*. 2009; 61:988–1006. [PubMed: 19643154]
25. Altman GH, Diaz F, Jakuba C, Calabro T, Horan RL, Chen JS, et al. Silk-based biomaterials. *Biomaterials*. 2003; 24:401–16. [PubMed: 12423595]
26. Wang Y, Kim HJ, Vunjak-Novakovic G, Kaplan DL. Stem cell-based tissue engineering with silk biomaterials. *Biomaterials*. 2006; 27:6064–82. [PubMed: 16890988]

27. Nagarkar S, Nicolai T, Chassenieux C, Lele A. Structure and gelation mechanism of silk hydrogels. *Phys Chem Chem Phys*. 12:3834–44. [PubMed: 20358077]
28. Wang X, Kaplan DL. Functionalization of Silk Fibroin with NeutrAvidin and Biotin. *Macromolecular bioscience*.
29. Nichol JW, Khademhosseini A. Modular tissue engineering: Engineering Biological Tissues from the Bottom Up. *Soft Matter*. 2009; 5:1312–19. [PubMed: 20179781]
30. Gobin AS, Froude VE, Mathur AB. Structural and mechanical characteristics of silk fibroin and chitosan blend scaffolds for tissue regeneration. *Journal of biomedical materials research*. 2005; 74:465–73. [PubMed: 15983992]
31. Venkataraman RGD, Singh SR, Pathak LC, Ghosh RN, Venkataraman B, Krishnamurthy R. Study on influence of porosity, pore size, spatial and topological distribution of pores on microhardness of as plasma sprayed ceramic coatings. *Materials Science and Engineering A*. 2007; 446:269–74.
32. Jiankang, He; Dichen, Li; Yaxiong, Liu; Bo, Yao; Bingheng, Lu; Qin, Lian. Fabrication and characterization of chitosan/gelatin porous scaffolds with predefined internal microstructures. *polymer*. 2007; 48:4578–88.
33. Gil ES, Frankowski DJ, Bowman MK, Gozen AO, Hudson SM, Spontak RJ. Mixed protein blends composed of gelatin and Bombyx mori silk fibroin: effects of solvent-induced crystallization and composition. *Biomacromolecules*. 2006; 7:728–35. [PubMed: 16529407]
34. Gil ES, Frankowski DJ, Spontak RJ, Hudson SM. Swelling behavior and morphological evolution of mixed gelatin/silk fibroin hydrogels. *Biomacromolecules*. 2005; 6:3079–87. [PubMed: 16283730]
35. Mandal BB, Mann JK, Kundu SC. Silk fibroin/gelatin multilayered films as a model system for controlled drug release. *European Journal of Pharmaceutical Sciences*. 2009; 37:160–71. [PubMed: 19429423]
36. Lv Q, Feng Q. Preparation of 3-D regenerated fibroin scaffolds with freeze drying method and freeze drying/foaming technique. *Journal of materials science*. 2006; 17:1349–56. [PubMed: 17143767]
37. Hyoung-Joon Jin JP, Karageorgiou Vassilis, Kim Ung-Jin, Valluzzi Regina, Cebe Peggy, Kaplan David L. Water-Stable Silk Films with Reduced  $\beta$ -Sheet Content. *Advanced Functional Materials*. 2005; 15:1241–7.
38. Wu X, Liu Y, Li X, Wen P, Zhang Y, Long Y, et al. Preparation of aligned porous gelatin scaffolds by unidirectional freeze-drying method. *Acta biomaterialia*. 6:1167–77. [PubMed: 19733699]
39. Bigi A, Cojazzi G, Panzavolta S, Rubini K, Roveri N. Mechanical and thermal properties of gelatin films at different degrees of glutaraldehyde crosslinking. *Biomaterials*. 2001; 22:763–8. [PubMed: 11246944]
40. Tomihata K, Ikada Y. Cross-linking of gelatin with carbodiimides. *Tissue Eng*. 1996; 2:307–13. [PubMed: 19877962]
41. Chen YS, Chang JY, Cheng CY, Tsai FJ, Yao CH, Liu BS. An in vivo evaluation of a biodegradable genipin-cross-linked gelatin peripheral nerve guide conduit material. *Biomaterials*. 2005; 26:3911–8. [PubMed: 15626438]
42. Chiono V, Pulieri E, Vozzi G, Ciardelli G, Ahluwalia A, Giusti P. Genipin-crosslinked chitosan/gelatin blends for biomedical applications. *Journal of materials science*. 2008; 19:889–98. [PubMed: 17665102]
43. Murtuza B, Nichol JW, Khademhosseini A. Micro- and nanoscale control of the cardiac stem cell niche for tissue fabrication. *Tissue Eng Part B Rev*. 2009; 15:443–54. [PubMed: 19552604]
44. Ifkovits JL, Burdick JA. Review: photopolymerizable and degradable biomaterials for tissue engineering applications. *Tissue Eng*. 2007; 13:2369–85. [PubMed: 17658993]
45. Wang X, Kluge JA, Leisk GG, Kaplan DL. Sonication-induced gelation of silk fibroin for cell encapsulation. *Biomaterials*. 2008; 29:1054–64. [PubMed: 18031805]
46. Yucel T, Cebe P, Kaplan DL. Vortex-induced injectable silk fibroin hydrogels. *Biophysical journal*. 2009; 97:2044–50. [PubMed: 19804736]
47. Nazarov R, Jin HJ, Kaplan DL. Porous 3-D scaffolds from regenerated silk fibroin. *Biomacromolecules*. 2004; 5:718–26. [PubMed: 15132652]

48. Gil ES, Spontak RJ, Hudson SM. Effect of beta-sheet crystals on the thermal and rheological behavior of protein-based hydrogels derived from gelatin and silk fibroin. *Macromolecular bioscience*. 2005; 5:702–9. [PubMed: 16080165]
49. Mandal BB, Kapoor S, Kundu SC. Silk fibroin/polyacrylamide semi-interpenetrating network hydrogels for controlled drug release. *Biomaterials*. 2009; 30:2826–36. [PubMed: 19203791]
50. Levental I, Georges PC, Janmey PA. Soft biological materials and their impact on cell function. *Soft Matter*. 2007; 3:299–306.
51. Moutos FT, Freed LE, Guilak F. A biomimetic three-dimensional woven composite scaffold for functional tissue engineering of cartilage. *Nature materials*. 2007; 6:162–7.
52. Freed LE, Guilak F, Guo XE, Gray ML, Tranquillo R, Holmes JW, et al. Advanced tools for tissue engineering: scaffolds, bioreactors, and signaling. *Tissue engineering*. 2006; 12:3285–305. [PubMed: 17518670]
53. Numata K, Cebe P, Kaplan DL. Mechanism of enzymatic degradation of beta-sheet crystals. *Biomaterials*. 2010; 31:2926–33. [PubMed: 20044136]
54. Li M, Ogiso M, Minoura N. Enzymatic degradation behavior of porous silk fibroin sheets. *Biomaterials*. 2003; 24:357–65. [PubMed: 12419638]
55. Du Y, Lo E, Ali S, Khademhosseini A. Directed assembly of cell-laden microgels for fabrication of 3D tissue constructs. *Proceedings of the National Academy of Sciences of the United States of America*. 2008; 105:9522–7. [PubMed: 18599452]

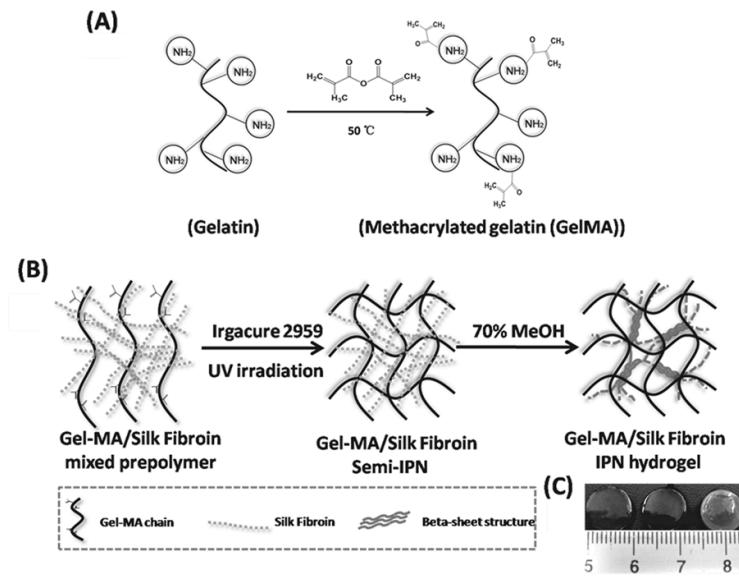


**Fig. 1.** Schematic for synthesizing gelatin methacrylate (GelMA), GelMA-SF composite semi-IPN and IPN hydrogels. Gelatin macromers containing primary amine groups were reacted with methacrylic anhydride (MA) to graft methacrylate pendant groups (A). To create the GelMA-SF IPN hydrogel, the gelatin methacrylate was mixed with SF solution and crosslinked by using UV irradiation in the presence of a photoinitiator, following treatment with 70% methanol (MeOH) was used to induce SF crystallization (B). Representative optical images of GelMA, G-S-1 semi-IPN, and G-S-1 IPN hydrogel (from left to right) (C)

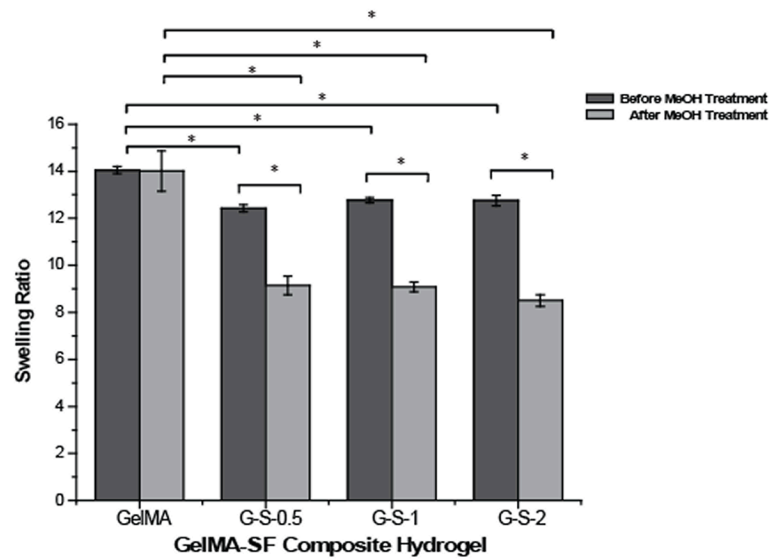


**Fig. 2.** The swelling property of GelMA-SF IPN, semi-IPN and pure GelMA hydrogels in DPBS (pH 7.4). Supplementing GelMA hydrogels (6 wt%) with SF (0.5, 1 and 2 wt%) generated GelMA-SF semi-IPN hydrogels that displayed a significant reduction in the swelling ratio ( $p < 0.05$ ). Treating GelMA-SF composite hydrogel with MeOH significantly reduced swelling ratios compared to GelMA-SF semi-IPN hydrogels at all SF concentrations ( $p < 0.05$ ). (\*) indicates significant difference with Fischer's LSD.

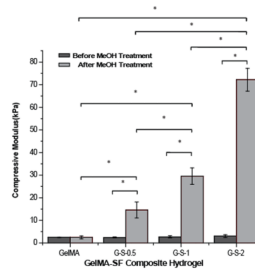


**Fig. 3.**

The compressive modulus of GelMA-SF IPN, semi-IPN and pure GelMA hydrogels. The addition of SF did not significantly alter the compressive modulus of GelMA-SF semi-IPN hydrogels when compared to GelMA alone. However, treatment with a 70% (v/v) MeOH solution significantly increased the compressive modulus of the GelMA-SF hydrogels compared to both GelMA alone and GelMA-SF semi-IPN hydrogels ( $p < 0.05$ ). (\*) indicates significant difference with Fischer's LSD.

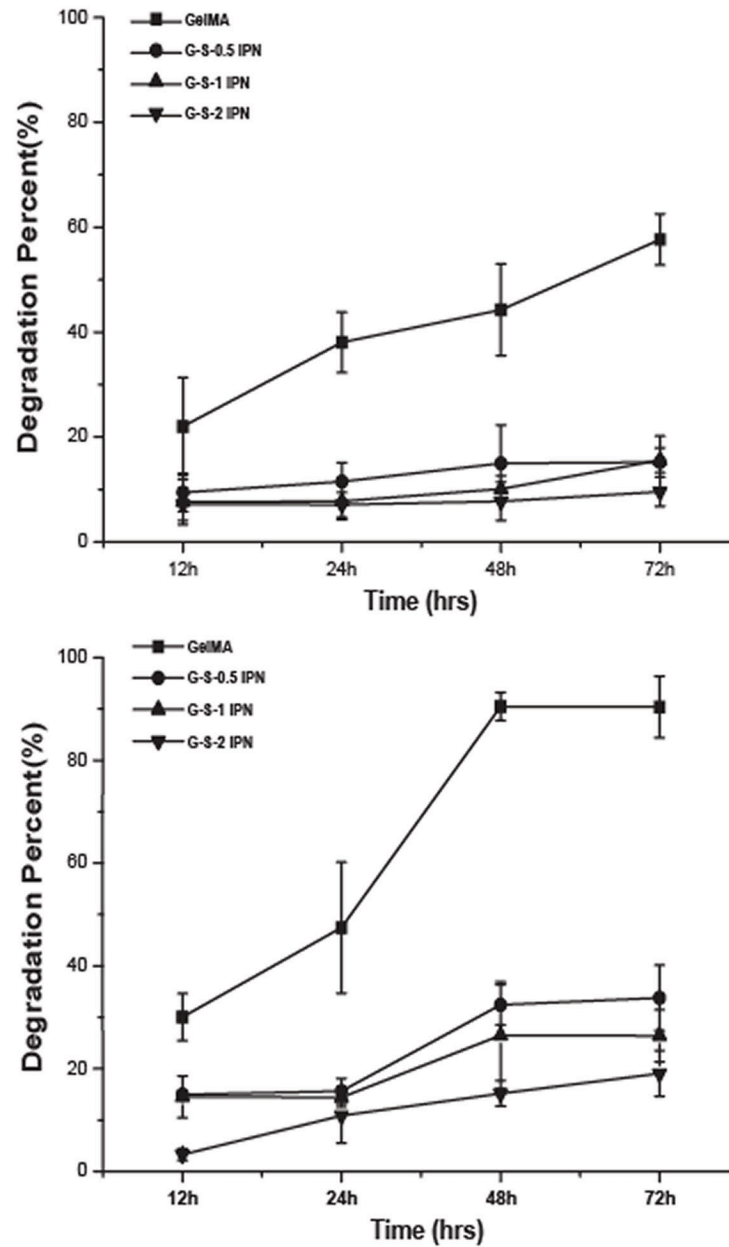


**Fig. 4.** Degradation profile of pure GelMA and GelMA-SF IPN hydrogel with different collagenase concentrations (1U/ml (A) and 2U/ml (B)). Overall, the addition of SF significantly reduced the degradation rate of GelMA-SF IPN hydrogels compared to GelMA alone ( $p < 0.05$ ). Furthermore, there was an inverse correlation between SF concentration and degradation rate of GelMA-SF IPN hydrogels.

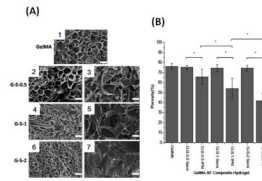


**Fig. 5.** SEM images of cross-section of GelMA hydrogels, GelMA-SF IPN and semi-IPN hydrogels (A). The structure of GelMA (A1) and semi-IPN (A2, A4, A6) were highly porous. For the IPN hydrogel (A3, A5, A7), the structure was more compact than semi-IPN and GelMA hydrogels. When the concentration of SF in IPN hydrogel was increased, flaky structures formed. The scale bars are 100 $\mu$ m. The porosity of the GelMA-SF composite hydrogels quantified by ImageJ based on the SEM images (B).

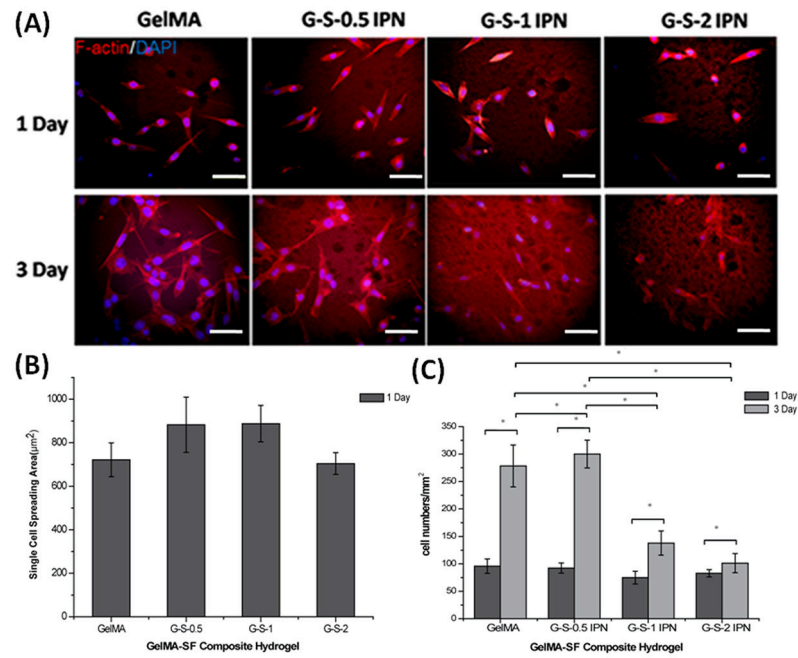


**Fig. 6.** Fluorescent images (20×) of NIH-3T3 cells on the hydrogel surface for days 1 and 3. The cytoskeletal F-actin fibers and nuclei were stained with rhodamine-labeled phalloidin and DAPI respectively (A). The single cell spreading area on the hydrogel surface after 1 day (B). The cell density on the hydrogel surface after 1 and 3 days (C). (\*) indicates significant difference with Fischer's LSD. The scale bars are 100 μm.

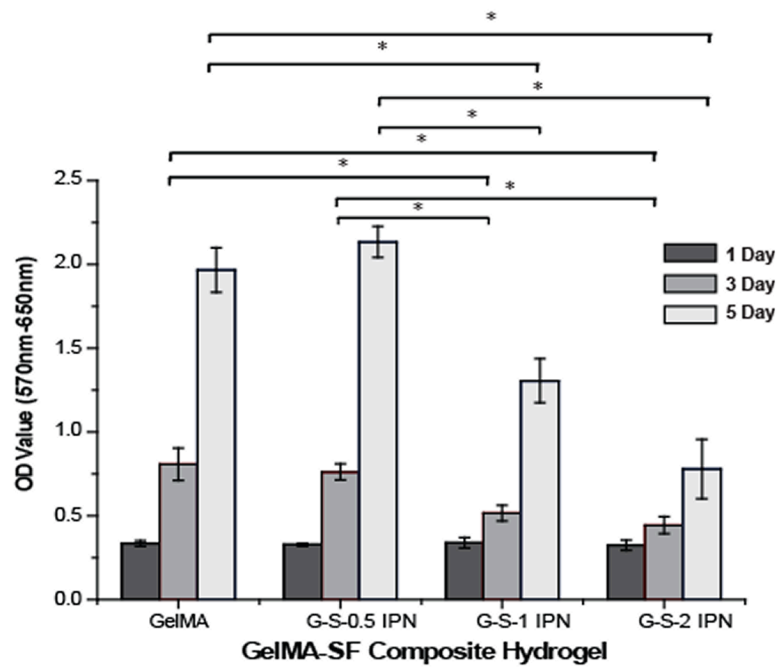


**Fig. 7.**

MTT analysis of the NIH-3T3 fibroblast seeded on the GelMA-SF IPN hydrogel surface after 1, 3 and 5 days. After 1 day in culture cell metabolic activity was statistically indistinguishable for all hydrogels. After 3 and 5 days of culture, MTT assay revealed the highest metabolic activities for pure GelMA hydrogels and GelMA-SF IPN with 0.5% SF ( $p < 0.05$ ). (\*) indicates significant difference with Fischer's LSD.

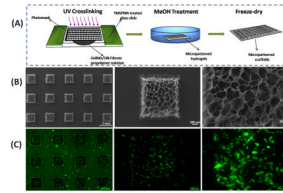


**Fig. 8.** Schematic of process to create micro-patterned scaffolds by photolithography and freeze-drying (A). The SEM images of micropatterned scaffold based on G-S-0.5 IPN hydrogel (B). Fluorescence images (2 $\times$ , 10 $\times$ , and 20 $\times$ ) of live/dead stained NIH-3T3 fibroblasts after seeded on the micropatterned scaffold for 1 day (C).

**Table 1**

The composition of GelMA-SF composite hydrogels and their nomenclature in the paper

| Sample  | GelMA (mg/ml) | Silk Fibroin (mg/ml) | Total (mg/ml) |
|---------|---------------|----------------------|---------------|
| GelMA   | 60            | 0                    | 60            |
| G-S-0.5 | 60            | 5                    | 65            |
| G-S-1   | 60            | 10                   | 70            |
| G-S-2   | 60            | 20                   | 80            |